Chemical Science

RSC Publishing

EDGE ARTICLE

View Article Online
View Journal | View Issue

Cite this: *Chem. Sci.*, 2013, **4**, 4212

Hetero-dehydrocoupling of silanes and amines by heavier alkaline earth catalysis†

Michael S. Hill,* David J. Liptrot, Dugald J. MacDougall, Mary F. Mahon and Thomas P. Robinson

Received 27th June 2013
Accepted 13th August 2013

DOI: 10.1039/c3sc51797g

www.rsc.org/chemicalscience

The homoleptic alkaline earth hexamethyldisilazides, $[M\{N(SiMe_3)_2\}_2]_2$ (**1**: M = Mg; **2**: M = Ca; **3**: M = Sr), have been demonstrated as active pre-catalysts for the cross-dehydrocoupling of Si–H and N–H bonds under mild (25–60 °C) conditions. The reactions are applicable to the coupling of a wide variety of amine and silane substrates and are proposed to occur *via* a sequence of discrete Si–H/M–N and N–H/M–H metathesis steps. Whereas reactions of dialkyl group 2 species with 2,6-di-*iso*-propylaniline and phenylsilane delivered a series of well-defined compounds consistent with this rationale, kinetic analysis of the cross-coupling of diethylamine with diphenylsilane provided evidence for a more complex and subtly variable mechanistic landscape. Although reactions performed with all three pre-catalysts presented a number of common features, in every case the calcium species, **2**, was found to provide notably superior catalytic activity, an order of magnitude higher than both **1** and **3** and in excess of many previously described benchmark transition metal- or f-element-mediated processes. Variations in overall reaction order, mode of pre-catalyst activation and the nature of the rate determining process are postulated to arise as a consequence of the marked change in M^{2+} radius and resultant charge density as group 2 is descended.

Introduction

The mediation of main group element–element (E–E) bond formation, particularly through the homo- and hetero-dehydrocoupling of E–H (or E′–H) bonds, is an enterprise that has commanded attention for over three decades.[1] As early as 1972 Keller demonstrated that more complex amidoboranes could be prepared by a combination of R_2N– for H exchange and H_2 elimination from the interaction of either lithium primary amides and B_2H_6 or alkali metal hydrides and amine boranes.[2] Driven by potential hydrogen storage applications, the dehydrocoupling of these latter species and ammonia borane has achieved recent prominence,[3] while recent advances describing a plethora of Si–Si,[4] P–P[1c,d,5] and B–B[6] bond forming reactions have signposted that a greatly enhanced generality for such bond construction processes may be within reach. Although an aggregate of these reports might suggest that the mediation of these processes is primarily the preserve of mid or late metals from the transition series, there is a growing awareness that main group elements selected from the s- and p-blocks of the periodic table may also provide comparable levels of small molecule reactivity.[7]

As archetypal main group compounds containing E–H bonds, hydrosilanes display diverse reactivity and have found application in a wide range of molecular and macromolecular homogeneous catalytic processes.[8] The hydrosilylation of C=X multiple bonds (X = C, N, O), for example, may be catalysed by a diverse array of transition and main group element species in which the mode of activation of the Si–H bond is determined by the nature of the catalytic metal centre.[9] Whereas oxidative addition pathways have been found to predominate for activation of the Si–H function by variable oxidation state transition metal compounds,[10] reactivity derived by the intermediacy of more electropositive d^0 main group or lanthanide species generally proceeds *via* polarized σ-bond metathesis pathways to provide metal hydrides together with a silicon-containing by-product.[11]

This reactivity may be elaborated to a catalytic regime through the introduction of a protic coupling partner E′–H, resulting in a net dehydrocoupling reaction and the formation of an E′–Si bond. In cases where E′–H represents an amine function (Scheme 1) this reactivity will expedite the formation of silylamines, valuable molecules which may be utilised as silylating agents,[12] bases[13] and ligands as well as polymer and ceramic precursors.[14] The synthesis of Si–N bonds is most commonly achieved through the aminolysis of chlorosilanes.[15] Consequently the dehydrogenative coupling of silanes and amines, obviating the production of HCl, has attracted significant attention. Heterogeneous catalysis has been achieved with several supported palladium systems[16] while a range of

Department of Chemistry, University of Bath, Claverton Down, Bath, BA2 7AY, UK. E-mail: msh27@bath.ac.uk

† Electronic supplementary information (ESI) available: Experimental procedures and characterisation data for all new compounds. CCDC 945785–945789. For ESI and crystallographic data in CIF or other electronic format see DOI: 10.1039/c3sc51797g

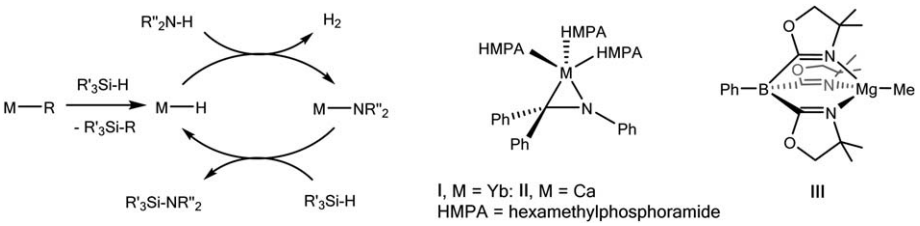

Scheme 1

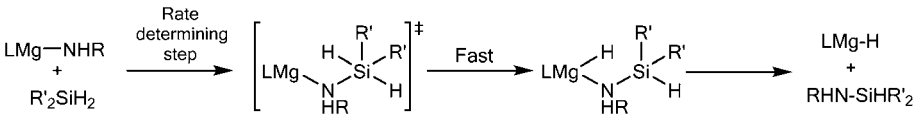

Scheme 2 Proposed mechanism for Si–N bond formation mediated by **III**.

titanium(IV),[17] chromium(III),[18] copper(I),[19] rhodium(I),[20] ruthenium(0),[21] ytterbium(II),[22] samarium(II)[22] and uranium(IV)[23] species have been identified for the homogeneous catalysis of this process. Although complexes of the heavier alkaline earth elements have an established pedigree as reagents for multiple bond heterofunctionalisation[24] and have recently been applied quite broadly in amine–borane[25] and to a lesser extent group 15 dehydrocoupling catalysis,[26] reports of group 2-mediated dehydrogenative silylamine synthesis are rather more limited. The first report of such an alkaline earth-promoted catalysis was provided by Harder and co-workers who,[27] inspired by the ytterbium ketamine derivative (**I**),[22a,b] utilised the isostructural calcium species (**II**) along with a dibenzyl calcium complex for the coupling of a variety of primary or secondary amines with Ph_3SiH or $Ph(Me)SiH_2$. In a similar manner Sadow has more recently demonstrated that the tris(oxazolinyl)boratomagnesium complex (**III**) may also act as a potent pre-catalyst for the dehydrocoupling of silane and amine (including ammonia and hydrazine) reaction partners.[28] The calcium-centred reactivity was proposed to occur through a sequential metathesis-based mechanism analogous to the process depicted in Scheme 1, while kinetic analysis of the dehydrocoupling reaction between $Ph(Me)SiH_2$ and $^tBuNH_2$ catalysed by **III** yielded the rate law shown as eqn (1).

$$\text{Rate} = k[\text{amine}]^0[\text{silane}]^1[\text{catalyst}]^1 \quad (1)$$

A large, negative entropy of activation, $\Delta S^{\ddagger}$, was supportive of a highly ordered transition state while kinetic isotope (k_H/k_D = 1.0(2)) and Hammett analyses supported only limited Si–H bond cleavage during the rate determining step of the reaction. These observations led Sadow to postulate the model presented in Scheme 2 in which nucleophilic attack of the magnesium amide on silane is followed by a rapid and energetically insignificant hydride transfer from the transient hypervalent silicon centre to yield the product neutral silazane complexed to magnesium.[28]

In this contribution we demonstrate that this catalytic silane–amine dehydrocoupling reactivity may be generalised to a self-consistent series of readily available heavier alkaline silylamide derivatives, $[M\{N(SiMe_3)_2\}_2]_2$ (M = Mg (**1**), Ca (**2**) and Sr (**3**)).[29] Through a combination of stoichiometric and catalytic studies we also provide a provisional mechanistic rationale for variations observed in activity and selectivity of these processes in relation to alkaline earth cation size, charge density and polarisation effects.

Results and discussion

Catalytic scope

An initial NMR investigation was undertaken into potential substrate scope for reactions catalysed by compounds **1–3** between the range of organosilanes and organic amines shown in Table 1. On addition of the pre-catalyst to a mixture of the amine and silane in C_6D_6 a pronounced bubbling was observed for many of the reactions. In general, hydrogen evolution occurred on mixing at room temperature, although some reactions required heating to 60 °C for the observation of appreciable product formation. While the available literature data and conditions applied in previous studies are somewhat disparate,[16–23,27,28] the requisite conditions for this group 2-catalysed dehydrogenative coupling are, at worst, commensurate with the best of the previously reported catalytic systems, for example Cui's recently described NHC-supported Yb(II) pre-catalyst,[22c] and are considerably milder than many of the late transition metal-based processes.

A number of notable general trends could be identified. Each of the pre-catalysts was found to be active for a wide range of both amine and silane coupling partners. Qualitatively, the calcium and strontium pre-catalysts, **2** and **3**, appeared to provide superior dehydrocoupling activity than their magnesium counterpart, **1**, while the reactivity survey indicated a clear kinetic dependence upon the relative steric demands of the amine and silane coupling partners. Triphenylsilane was almost entirely inactive with magnesium (Table 1, entries 13–18), providing only modest yields of the silazane products with the least bulky amines, *n*-benzylamine (Table 1, entry 13) and pyrrolidine (Table 1, entry 16). The dehydrocoupling of primary

Table 1 The scope of silicon–nitrogen dehydrocoupling catalysed by complexes **1–3**

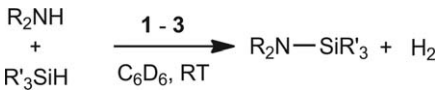

Entry	Catalyst[c]	Silane	Amine	Product	Conversion/%
1	**1**	$PhSiH_3$	$BnNH_2$	Intractable mixture	99[a]
2			$^tBuNH_2$	$PhSiH_2NH^tBu + PhSiH(NH^tBu)_2$	99 (86 : 14)[a]
3			$DippNH_2$[d]	$PhSiH_2NHDipp + PhSiH(NHDipp)_2$	99 (39 : 61)[a]
4			$(CH_2)_4NH$	$PhSiH_2(N(CH_2)_4) + PhSiH(N(CH_2)_4)_2$	99 (29 : 71)[a]
5			$EtNH_2$	$PhSiH_2NEt_2 + PhSiH(NEt_2)_2$	99 (99 : trace)[a]
6			$(Me_3Si)_2NH$	$PhSiH_2N(SiMe_3)_2$	71[a]
7		Ph_2SiH_2	$BnNH_2$	$Ph_2SiHNHBn + Ph_2Si(NHBn)_2$	99 (97 : 3)[a]
8			$^tBuNH_2$	Ph_2SiHNH^tBu	95[b]
9			$DippNH_2$[d]	$Ph_2SiHNHDipp$	99[a]
10			$(CH_2)_4NH$	$Ph_2SiHN(CH_2)_4$	99[a]
11			Et_2NH	$Ph_2SiHNEt_2$	99[a]
12			$(Me_3Si)_2NH$	No reaction	0[b]
13		Ph_3SiH	$BnNH_2$	$Ph_3SiNHBn$	25[b]
14			$^tBuNH_2$	No reaction	0[b]
15			$DippNH_2$[d]	No reaction	0[b]
16			$(CH_2)_4NH$	$Ph_3SiN(CH_2)_4$	7[b]
17			Et_2NH	No reaction	0[b]
18			$(Me_3Si)_2NH$	No reaction	0[b]
19	**2**	$PhSiH_3$	$BnNH_2$	Intractable mixture	99[a]
20			$^tBuNH_2$	$PhSiH_2NH^tBu + PhSiH(NH^tBu)_2 + (PhSiH_2)_2N^tBu$	99 (78 : 10 : 12)[a]
21			$DippNH_2$[d]	$PhSiH_2NHDipp + PhSiH(NHDipp)_2 + (PhSiH_2)_2NDipp$	99 (12 : 20 : 68)[a]
22			$(CH_2)_4NH$	$PhSiH(N(CH_2)_4)_2$	99[a]
23			$EtNH_2$	$PhSiH_2NEt_2 + PhSiH(NEt_2)_2$	99 (87 : 13)[a]
24			$(Me_3Si)_2NH$	$PhSiH_2N(SiMe_3)_3$	99[a]
25		Ph_2SiH_2	$BnNH_2$	$Ph_2SiHNHBn + Ph_2Si(NHBn)_2 + (PhSiH)_2NBn$	99 (80 : 12 : 8)[a]
26			$^tBuNH_2$	Ph_2SiHNH^tBu	99[a]
27			$DippNH_2$[d]	$Ph_2SiHNHDipp$	99[a]
28			$(CH_2)_4NH$	$Ph_2SiHN(CH_2)_4$	94 (98 : 2)[a]
29			$EtNH_2$	$Ph_2SiHNEt_2$	88[a]
30			$(Me_3Si)_2NH$	No reaction	0[a]
31		Ph_3SiH	$BnNH_2$	$Ph_3SiNHBn$	99[a]
32			$^tBuNH_2$	Ph_3SiNH^tBu	7[b]
33			$DippNH_2$[d]	No reaction	0[b]
34			$(CH_2)_4NH$	$Ph_3SiN(CH_2)_4$	99[b]
35			Et_2NH	Ph_3SiNEt_2	54[b]
36			$(Me_3Si)_2NH$	No reaction	0[b]
37	**3**	$PhSiH_3$	$BnNH_2$	Intractable mixture	99[a]
38			$^tBuNH_2$	$PhSiH_2NH^tBu + PhSiH(NH^tBu)_2$	99 (58 : 42)[a]
39			$DippNH_2$[d]	$PhSiH_2NHDipp\ (PhSiH_2)_2NDipp$	99 (31 : 33)[a,e]
40			$(CH_2)_4NH$	$PhSiH_2(N(CH_2)_4) + PhSiH(N(CH_2)_4)_2$	99 (15 : 85)[a]
41			$EtNH_2$	$PhSiH_2NEt_2 + PhSiH(NEt_2)_2$	96 (89 : 11)[a]
42		Ph_2SiH_2	$BnNH_2$	$Ph_2SiHNHBn + Ph_2Si(NHBn)_2 + (PhSiH)_2NBn$	99 (5 : 35 : 55)[a,e]
43			$DippNH_2$[d]	$Ph_2SiHNHDipp + (Ph_2SiH)_2NDipp$	99 (77 : 23)[a]
44		Ph_3SiH	$BnNH_2$	$Ph_3SiNHBn$	99[a]
45			$^tBuNH_2$	Ph_3SiNH^tBu	54[b]
46			$DippNH_2$[d]	No reaction	0[b]
47			$(CH_2)_4NH$	$Ph_3SiN(CH_2)_4$	91[a]
48			Et_2NH	Ph_3SiNEt_2	83[b]
49			$(Me_3Si)_2NH$	No reaction	0[b]

[a] Reaction performed at room temperature. [b] Reaction performed at 60 °C. [c] Reactions performed at 5 mol% catalyst loading. [d] Dipp = 2,6-di-*iso*-propylphenyl. [e] Higher oligomers constitute the remainder of the conversion.

amines of low to moderate steric demands with all three silane partners was readily catalysed by each of the group 2 species (Table 1, entries 1–3, 7–9, 19–21, 25–27, 31, 37–39, 42–44) with the exception of the aforementioned issues with magnesium. The bulkiest amine, 2,6-di-*iso*-propylaniline, however, could not be dehydrocoupled with the most sterically encumbered silane, Ph_3SiH, by any of the group 2 pre-catalysts (Table 1, entries 15, 33, 46). This sterically demanding aniline did, however, provide high activity with the less sterically congested phenylsilane (*vide infra*), yielding doubly dehydrocoupled products and higher oligomers in preference to single dehydrocoupling irrespective of the reaction stoichiometry (Table 1, entries 3, 21, 39). The sterically demanding primary aliphatic amine, *tert*-butylamine, also provided only poor yields in dehydrocoupling reactions with Ph_3SiH catalysed by **2** and **3** (Table 1, entries 32, 45). These observations suggest that both the steric demands and electronic character (nucleophilicity/basicity) of the amine substrate exert a significant influence on reactivity with, in contrast to dehydrocoupling reactions mediated by **III**,[28] the far more acidic aniline coupling more readily than its aliphatic partners where the bulk of the silane coupling partner is insignificant.

Secondary amines of low steric demands were readily dehydrocoupled, with pyrrolidine providing more facile reactivity than its less basic acyclic analogue diethylamine with phenylsilane (Table 1, entries 4, 5, 23, 24, 40, 41). This enhanced reactivity, however, resulted in lower selectivity with the doubly dehydrocoupled $PhSiH(N(CH_2)_4)_2$ forming in preference to the singly dehydrocoupled $PhSiH_2(N(CH_2)_4)$ when this amine was combined with phenylsilane for all three pre-catalysts. Although very bulky secondary amines such as hexamethyldisilazane provided some limited reactivity with the less sterically congested phenylsilane (Table 1, entries 6, 24), the more substituted di- and triphenylsilane provided no reaction (Table 1, entries 12, 18, 30, 36, 49). Consistently high conversions were otherwise observed, indicating a set of broadly active pre-catalysts with good tolerance for a variety of substrates and reasonable activity under mild conditions.

Finally, multiple dehydrocoupling to yield bis- and tris-aminosilanes or bis-silylamines was observed particularly for phenylsilane (Table 1, entries 1–5, 19–21, 23, 37–41). The least sterically congested pairing of phenylsilane and benzylamine rapidly and consistently yielded intractable mixtures of higher oligomers suggesting that subsequent dehydrocoupling of the initially formed silazane, $PhSiH_2N(H)Bz$ is very rapid for all metals with these substrates (Table 1, entries 1, 19, 37). Furthermore, the strontium pre-catalyst **3** yielded higher oligomers with phenylsilane and the highly active 2,6-di-*iso*-propylaniline (Table 1, entry 39) and also through the combination of benzylamine with diphenylsilane (Table 1, entry 42). Pre-catalyst **3** also provided multiple silane substitution in all dehydrocoupling reactions involving either phenyl- or diphenylsilane (Table 1, entries 37–43). The rational synthesis of more substituted silazane species was, thus, investigated by NMR spectroscopy utilising amine to silane ratios reflective of the stoichiometries of the desired heavier aminosilane

Table 2 Group 2-catalysed silicon–nitrogen dehydrocoupling to yield higher silazanes

Entry	Catalyst[c]	Silane	Amine	Ratio	Product	Conversion/%
1	**1**	$PhSiH_3$	$BnNH_2$	1 : 3	$(BnNH)_3SiPh + (BnNH)_2SiHPh$	99 (91 : 9)[a]
2			$^tBuNH_2$	1 : 2	$PhSiH_2NH^tBu + PhSiH(NH^tBu)_2$	92 (77 : 23)[a]
3			$(CH_2)_4NH$	3 : 1	$PhSiH_2(N(CH_2)_4) + PhSiH(N(CH_2)_4)_2$	66 (100 : 0)[b]
4				1 : 2		99 (84 : 16)[a]
5		Ph_2SiH_2	$BnNH_2$	1 : 2	$Ph_2SiHNHBn + Ph_2Si(NHBn)_2$	90 (30 : 70)[a]
6				2 : 1		99 (99 : trace)[a]
7			$^tBuNH_2$	1 : 2	Ph_2SiHNH^tBu	64[b]
8				2 : 1		99[b]
9			$(CH_2)_4NH$	1 : 2	$Ph_2SiHN(CH_2)_4 + Ph_2Si(N(CH_2)_4)_2$	55 (83 : 17)[b]
10	**2**		$BnNH_2$	1 : 3	Intractable mixture	99[a]
11			$^tBuNH_2$	1 : 3	$PhSiH(NH^tBu)_2 + (PhSiH_2)_2N^tBu$	66 (100 : 0)[b,d]
12				1 : 2		87 (93 : 7)[a]
13				2 : 1		99 (0 : 100)[a]
14			$(CH_2)_4NH$	3 : 1	$PhSiH(N(CH_2)_4)_2 + PhSi(N(CH_2)_4)_3$	99 (0 : 100)[b]
15				1 : 2		99 (100 : 0)[a]
16		Ph_2SiH_2	$BnNH_2$	1 : 2	$Ph_2SiHNHBn + Ph_2Si(NHBn)_2 +$	99 (0 : 100 : 0)[a]
17				2 : 1	$(Ph_2SiH)_2NBn$	99 (52 : 9 : 39)[a]
18			$^tBuNH_2$	1 : 2	$Ph_2SiHNH^tBu + Ph_2Si(NH^tBu)_2$	99 (65 : 35)[b]
19				2 : 1		99 (100 : 0)[b]
20			$(CH_2)_4NH$	1 : 2	$Ph_2SiHN(CH_2)_4 + Ph_2Si(N(CH_2)_4)_2$	95 (12 : 88)[a]
21	**3**	$PhSiH_3$	$^nBnNH_2$	1 : 3	Intractable mixture	99[a]
22			$^tBuNH_2$	1 : 3	$PhSiH(NH^tBu)_2$	66[a,d]
23				1 : 2		99[a,d]
24			$(CH_2)_4NH$	3 : 1	$PhSi(N(CH_2)_4)_3$	99[b]
25		Ph_2SiH_2	$BnNH_2$	1 : 2	$Ph_2Si(NHBn)_2 + (Ph_2SiH)_2NBn$	99 (88 : 12)[a]
26				2 : 1		99 (100 : 0)[a]

[a] Reaction performed at room temperature. [b] Reaction performed at 60 °C. [c] Reactions performed at 5 mol% catalyst loading. [d] Higher oligomers constitute the remainder of the conversion.

oligomers. The information provided in Table 2 summarises the outcome of these studies.

Poly-substituted silazanes were found to be generally accessible, although conversion of the mono-substituted products appeared to occur less readily than the initial dehydrocoupling. Given the bulk-sensitive nature of these reactions and the effect of aminosilane formation on the hydridicity of silicon–hydrogen bonds this is unsurprising. Of particular note was the reaction of benzylamine with phenylsilane in a 3 : 1 ratio catalysed by the magnesium pre-catalyst **3**, which yielded well-defined tri-and di-substituted products in contrast to the results of the 1 : 1 reaction (Table 2, entry 1). The heavier congener pre-catalysts **2** and **3**, however, again yielded intractable products (Table 2, entries 10, 21). Reactions performed at a 1 : 3 phenylsilane : amine ratio provided access to the tris-aminated products for amines with lower overall steric demands (Table 2, entries 1, 14, 24; *cf.* entries 3, 11, 22). Although bis(amino)-silanes were accessible from use of initial 1 : 2 silane : amine ratios, these products only formed cleanly in a limited number of cases (Table 2, entries 11, 15, 26) and only for pre-catalysts **2** and **3** derived from the heavier alkaline earth metals, Ca and Sr. With bulkier amines the singly dehydrocoupled product was generally favoured (Table 2, entries 2, 4, 9, 15, 23), irrespective of the reaction stoichiometry. Aside from a few notable exceptions (Table 2, entries 13, 17, 25), where they were observed to form as a small proportion of the product mixture, disilyl-amines, targeted from reactions performed with 2 : 1 silane : amine ratios, were generally inaccessible.

This study demonstrated that amine–silane dehydrocoupling is readily catalysed by group 2 amides under mild conditions giving moderate to excellent conversions for a broad range of coupling partners. A number of trends may also be discerned. Both the steric demands and the electronic character of both coupling partners have a significant influence on reactivity. The degree to which steric bulk influences the reaction is profoundly influenced by the size of the metal centre; effects are smallest on strontium and largest on magnesium. This has an effect both on the reactions of bulky amines and silanes and also multiple dehydrocouplings to yield bis(amino)silanes. In contrast to the observations of Sadow and co-workers,[28] more acidic anilines were generally found to undergo dehydrocoupling more readily than aliphatic amines, suggestive of a contrasting mechanism. These empirical studies also indicated that strontium and calcium appear to provide significantly higher activity than magnesium as evidenced by both their shorter reaction times and milder conditions, but notably reduced selectivity.

Stoichiometric studies

The catalytic formation of the product compounds listed in Tables 1 and 2 is predicated upon a sequence of N–H/M–H dihydrogen elimination and Si–H/M–N silicon–nitrogen bond forming reactions (Scheme 1). We, thus, undertook a series of stoichiometric reactions in an attempt to provide direct evidence of such metal-centred reactivity through the isolation of possible group 2-containing intermediate species. In order to avoid complications resulting from the presence of liberated $HN(SiMe_3)_2$ (*vide infra*) the alkyl reagents, commercially available di-butylmagnesium, **4**, and the calcium and strontium dialkyl species $[M\{CH(SiMe_3)_2\}_2(THF)_2]$ (**5**, M = Ca; **6**, M = Sr),[30] were employed in place of the amide pre-catalysts **1–3** utilised in the earlier catalytic study.

An initial room temperature reaction between a 1 : 1 : 2 mixture of di-butylmagnesium, phenylsilane and 2,6-di-*iso*-propylaniline in heptanes yielded the doubly dehydrocoupled species DippNHSiPh(H)NHDipp, **7**, (Dipp = 2,6-di-*iso*-propyl-phenyl) as the only isolable compound after separation of the reaction mixture from a finely dispersed colourless solid by filtration. Crystals of **7** suitable for analysis by single crystal X-ray diffraction were grown direct from the filtered solution and the results of this analysis are shown in Fig. 1. Details of the analysis and selected bond length and angle data are provided in Tables 3–5 respectively.

In contrast, a repeat of this reaction performed in THF provided, by fractional crystallisation from toluene at reduced temperature, both the magnesium-anilide–silylanilide **8** and the magnesium bis(amido)silane **9**. Compounds **8** and **9** were identified by mechanical separation of the two types of crystals and subsequent X-ray diffraction analysis. The structures of these species are shown in Fig. 2 and 3 respectively while details of the X-ray analysis and selected bond length and angle data are summarised in Tables 3–5.

The formation of compounds **8** and **9** evidently occurs competitively and we, thus, surmise that the production of these magnesium species along with the conjugate acid **7** may be accounted for by the stepwise series of Si–H and N–H metathesis reactions depicted in Scheme 3. In this case an initially formed, but unobserved, magnesium bis-anilide

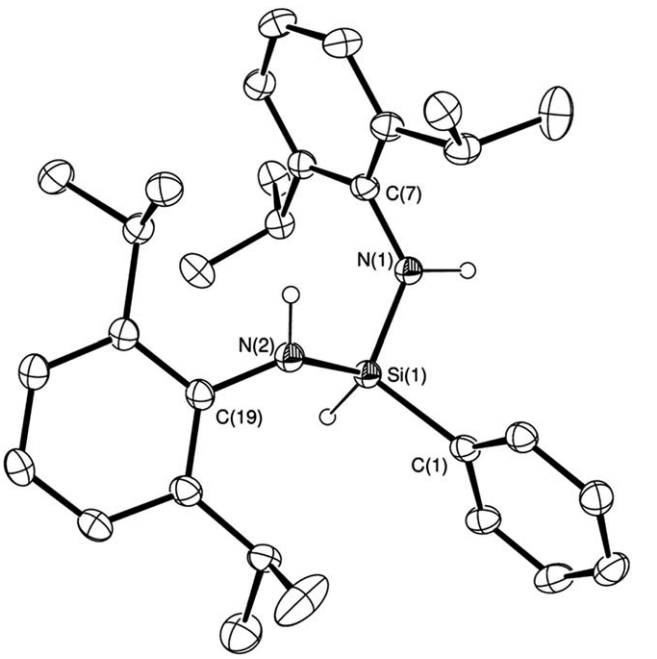

Fig. 1 ORTEP representation of compound **7**. Thermal ellipsoids at 30% probability and hydrogen atoms, except those attached to N(1), Si(1) and N(2), omitted for clarity.

Table 3 Crystallographic analyses of compounds **7–11**

	7	8	9	10	11
Molecular formula	$C_{30}H_{42}N_2Si$	$C_{38}H_{58}MgN_2O_2Si$	$C_{44}H_{68}MgN_2O_{3.5}Si$	$C_{49}H_{72}CaN_2O_3Si$	$C_{46}H_{71}N_2O_4SiSr$
Formula weight (g mol^{-1})	458.75	627.26	733.40	805.26	831.76
Crystal system	Monoclinic	Triclinic	Monoclinic	Monoclinic	Monoclinic
Space group	$P2_1/a$	$P\bar{1}$	$P2_1/n$	$P2_1/n$	$P2_1$
a (Å)	15.1354(4)	11.2940(4)	10.0310(1)	10.2642(2)	10.3700(3)
b (Å)	9.2400(3)	12.1680(4)	30.0170(5)	22.7621(6)	18.8520(8)
c (Å)	20.1280(6)	13.6040(4)	16.5560(3)	20.7835(5)	12.6320(5)
α (deg)	90	96.759(2)	90	90	90
β (deg)	101.781(2)	90.610(2)	104.903(1)	98.249(2)	113.60(2)
γ (deg)	90	90.961(2)	90	90	90
V (Å^3)	2755.63(14)	1856.13(10)	4817.34(13)	4805.5(2)	2262.83(15)
Z	4	2	4	4	2
μ (mm^{-1})	0.105	0.113	0.098	0.195	1.260
ρ (g cm^{-3})	1.106	1.122	1.011	1.113	1.221
θ range (°)	3.81 to 27.48	3.53 to 27.49	3.62 to 27.44	5.04 to 25.03	3.68 to 27.52
$R1$, w$R2$ [$I > 2\sigma(I)$]	0.0578, 0.1372	0.0612, 0.1597	0.0815, 0.2128	0.0756, 0.1990	0.0640, 0.119
$R1$, w$R2$ (all data)	0.0757, 0.1484	0.989, 0.1843	0.1607, 0.2434	0.1379, 0.2270	0.1090, 0.1238
Measured/independent reflections/R_{int}	35 403/6254/0.0772	25 602/8357/0.0590	10 746/10 746/0.0000	64 099/8386/0.1702	37 584/10 228/0.1217

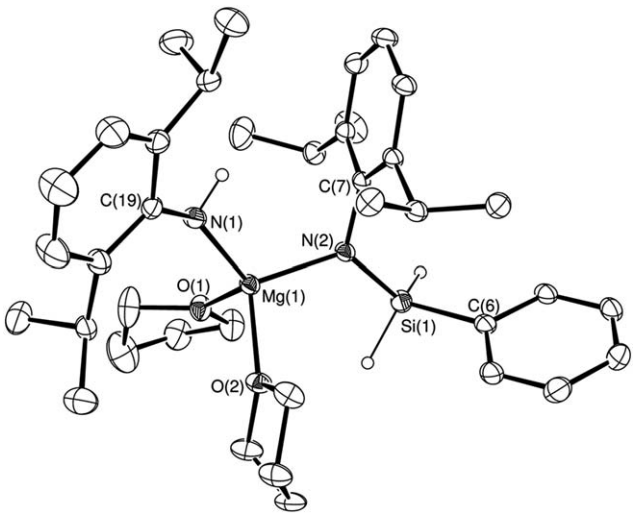

Fig. 2 ORTEP representation of compound **8**. Thermal ellipsoids at 30% probability. Minor disordered fractional atoms and hydrogen atoms, except those attached to N(1) and Si(1), omitted for clarity.

undergoes Si–H metathesis with formation of the silylated aniline DippN(H)SiH_2Ph and an anildomagnesium hydride. These latter species have not been isolated but can either immediately undergo self-protonolysis to form compound **8** and dihydrogen or engage in further Si–H/Mg–N metathesis to produce compound **7** and MgH_2, which precipitates for reactions performed in heptanes but which may themselves eliminate dihydrogen to provide compound **9** when performed in the more solubilising medium of THF (route A in Scheme 3). Alternatively, compound **8** may itself engage in intramolecular Si–H/Mg–N metathesis with subsequent H_2 elimination *via* the resultant magnesium hydride (route B). Although we have not fully identified the conditions which may be employed to maximise the production of either the magnesium compounds **8** and **9** or compound **7**, and irrespective of the precise order of compound formation, these observations provide clear evidence of the viability of the individual reaction steps illustrated by Scheme 1 and a stepwise mechanism for the magnesium-catalysed silane/amine dehydrocoupling reactions compiled in Tables 1 and 2.

In a similar manner, reactions between a 1 : 1 : 2 mixture of either of the heavier alkaline earth alkyl compounds, **5** or **6**, with phenylsilane and 2,6-di-*iso*-propylaniline in THF produced a rapid exotherm and immediate foaming of the solution (Scheme 4). In both cases, evaporation and low temperature crystallisation of the resulting solids from toluene solution yielded crystals of compounds **10** and **11** suitable for single crystal X-ray diffraction analysis. The results of the structural

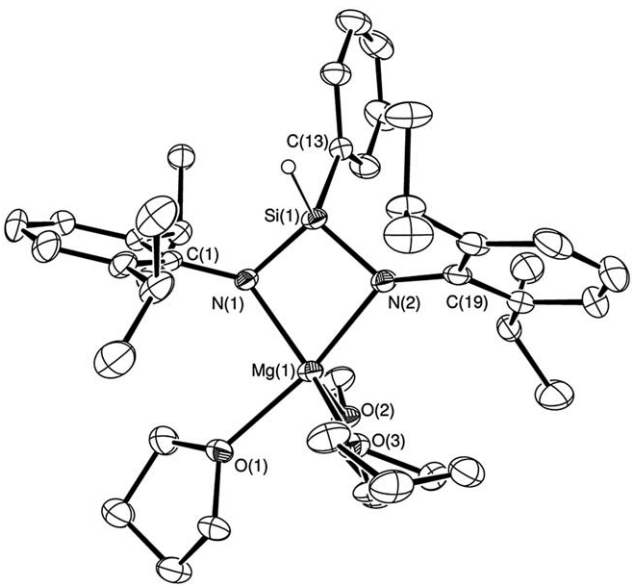

Fig. 3 ORTEP representation of compound **9**. Thermal ellipsoids at 30% probability. Minor disordered fractional atoms and hydrogen atoms, except for that attached to Si(1), omitted for clarity.

Table 4 Selected bond lengths (Å) for compounds **7–11**

	7	8[a]	9[a]	10[b]	11[c]
M(1)–N(1)	—	1.9795(19)	2.044(2)	2.281(3)	2.489(4)
M(1)–N(2)	—	2.0073(18)	2.108(3)	2.342(3)	2.494(4)
M(1)–O(1)	—	2.0341(1)	2.157(2)	2.335(3)	2.591(3)
M(1)–O(2)	—	2.0194(16)	2.057(2)	2.377(3)	2.597(3)
M(1)–O(3)	—	—	2.075(2)	2.388(3)	2.645(3)
M(1)–O(4)	—	—	—	—	2.561(4)
N(1)–Si(1)	1.7119(16)	—	1.699(3)	1.699(3)	1.704(4)
N(2)–Si(1)	1.7281(17)	1.6908(18)	1.696(2)	1.693(3)	1.693(4)

[a] M = Mg. [b] M = Ca. [c] M = Sr.

determinations are illustrated in Fig. 4 and 5 and reveal compounds **10** and **11** to be the respective calcium and strontium analogues of the magnesium bis(amido)silane, compound **9**. Although the data collected from crystals of compound **10** was of low quality [R(int) = 0.1702], the connectivity was unambiguous and details of both analyses and selected bond length and angle data are, thus, included for purposes of comparison in Tables 3–5 respectively.

While the bond lengths and angles in the group 2 amide complexes **8–11** are generally unremarkable and comparable to previously reported amide,[31] silylamide[29,32] and bis(amido)-silane[33] derivatives of Mg, Ca or Sr, the constitutions of compound 7 and the dianionic ligand formed by its deprotonation in compounds **9–11** are unprecedented for any metal complex in containing a bridging Si–H function between the two nitrogen centres. The increase of M^{2+} radius with group 2 atomic weight is reflected by the M–N bond lengths of compounds **9** (M = Mg, 2.044(2), 2.108(3) Å), **10** (M = Ca, 2.281(3), 2.342(3) Å), and **11** (M = 2.489(4), 2.494(4) Å) as well as the number of molecules of coordinated THF which raise the alkaline earth coordination number from five for compounds **9** and **10** to six for compound **11**.

Mechanistic considerations

The dehydrocoupling reaction of diethylamine with diphenylsilane catalysed by the metal silylamides **1–3** (Scheme 5) was selected for more detailed analysis due to its appropriate reaction kinetics and well-defined products which provide readily identifiable resonances in ^{1}H NMR spectra. NMR solutions were prepared in the glovebox and immediately cooled to 193 K on removal before being warmed to 298 K within the spectrometer. Concentrations of substrate and product were monitored by integration over three half-lives in comparison to a tetrakis-(trimethylsilyl)silane standard, added at the end of the run.

Consistent with the expectation provided by the earlier observations of silane–amine dehydrocoupling catalysis (Tables 1 and 2) the calcium-based pre-catalyst **2** provided a turnover frequency (TOF) that was more than an order of magnitude higher than either the analogous magnesium or strontium species (Table 6).

Catalysis of the reactions shown in Scheme 4 with both the magnesium and calcium silylamides, **1** and **2**, was found to proceed with first order first order kinetics over a 5–10 mol% range of [**1**] and [**2**], while further *pseudo*-first order experiments, in which tenfold excesses of silane were reacted with single equivalents of amine and *vice versa*, yielded zero and first order dependences on [Ph_2SiH_2] and [Et_2NH] respectively. The rate laws for both the magnesium- and calcium-catalysed reactions were thus deduced to be of the form

$$-\frac{\mathrm{d}[\mathrm{amine}]}{\mathrm{d}t}(\mathbf{1},\ \mathbf{2}) = k[\mathrm{cat}]^1[\mathrm{amine}]^1[\mathrm{silane}]^0 \qquad (2)$$

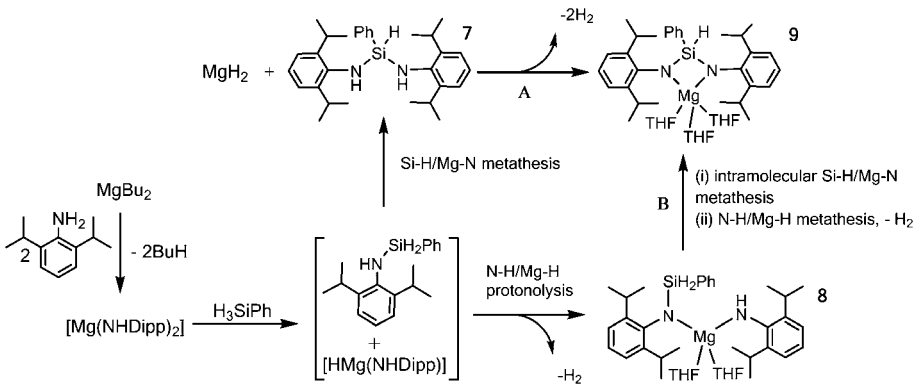

Scheme 3

Scheme 4

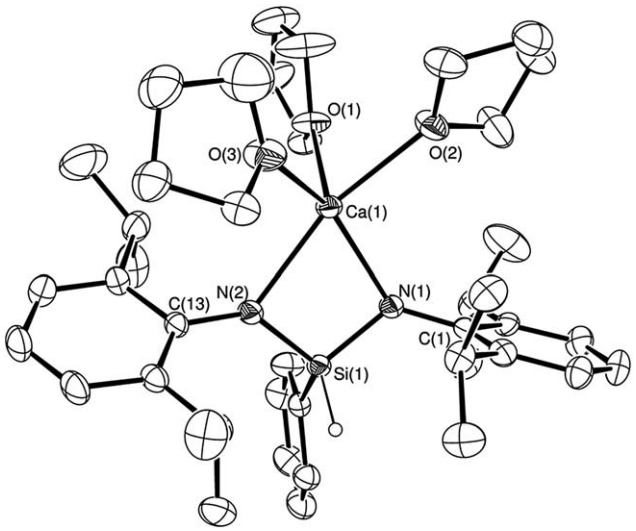

Fig. 4 ORTEP representation of compound **10**. Thermal ellipsoids at 30% probability. Minor disordered fractional atoms and hydrogen atoms, except for that attached to Si(1), omitted for clarity.

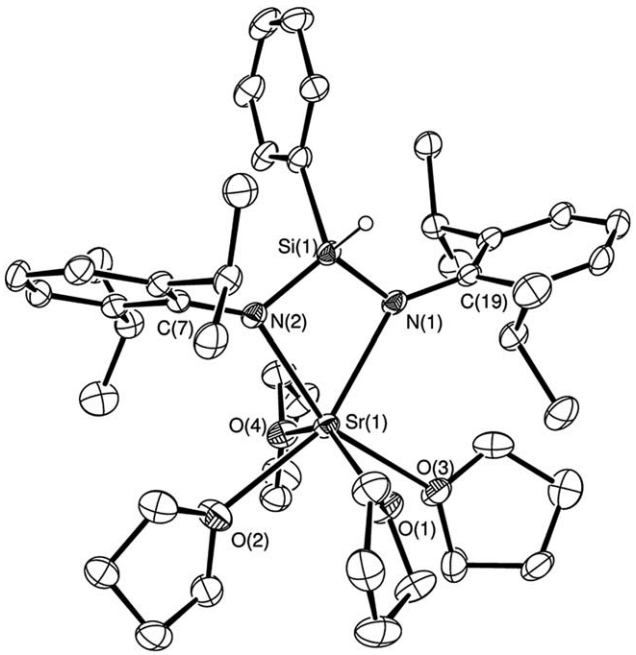

Fig. 5 ORTEP representation of compound **11**. Thermal ellipsoids at 30% probability. Minor disordered fractional atoms and hydrogen atoms, except for that attached to Si(1), omitted for clarity.

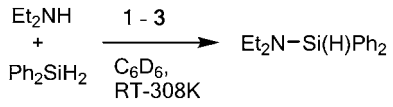

Scheme 5

Assuming that eqn (2) reflects an elementary reaction step and correlates with molecularity in the catalysis, these rate laws are suggestive of a turnover-limiting process involving one molecule of amine and a single magnesium or calcium catalytic centre. In contrast, a zero order dependence on [silane] appears to indicate that Ph_2SiH_2 plays no role in the rate-determining process. Similar experiments performed with compound **3** revealed that the strontium-based catalysis displayed divergent behaviour, providing second order rate constants as a consequence of first order dependences on both [Et_2NH] and [Ph_2SiH_2]. A second order dependence on [**3**] was also deduced indicating the rate law shown as eqn (3) for the strontium catalysis.

$$-\frac{\mathrm{d}[\mathrm{amine}]}{\mathrm{d}t}(\mathbf{3}) = [\mathrm{cat}]^2[\mathrm{amine}]^1[\mathrm{silane}]^1 \quad (3)$$

Additional insight into the course of these reactions was provided by monitoring of ^{1}H NMR spectra obtained from a further series of reactions between a 1 : 1 ratio of diethylamine and diphenylsilane in the presence of 5 mol% **1–3**. Whereas only *ca.* 50% of the Mg–N(SiMe$_3$)$_2$ environments of **1** were consumed during the catalytic reaction, with production of $Ph_2SiHN(SiMe_3)_2$ and a smaller quantity (*ca.* 5% by ratio) of $HN(SiMe_3)_2$, both of the heavier congeners, compounds **2** and **3**, were observed to undergo complete consumption of any calcium- or strontium-bound hexamethyldisilazide residues. In these latter cases, catalyst initiation occurred with complete conversion either to the product of Si–H/M–N metathesis, $Ph_2SiHN(SiMe_3)_2$, or N–H/M–N protonolysis, $HN(SiMe_3)_2$, for **2** and **3** respectively. In the case of **2**, this exclusive, irreversible metathesis-based activation yields a brief induction period which initially complicated kinetic analysis. As a result of this, premixing of the precatalyst, **2**, and diphenylsilane was utilised to deconvolute the kinetics, rendering them amenable to analysis.

We have previously reported that the efficacy of group 2-catalysed alkene hydroamination is heavily influenced by the ability of the amine substrate to enter the catalytic manifold and

Table 5 Selected bond angles (°) for compounds **7–11**

	7	**8**[a]	**9**[a]	**10**[b]	**11**[c]
N(1)–M(1)–N(2)	—	114.07(8)	77.15(10)	69.46(12)	65.04(12)
N(1)–M(1)–O(1)	—	112.31(8)	96.05(10)	109.10(12)	107.00(12)
N(2)–M(1)–O(1)	—	110.04(8)	164.22(10)	114.58(13)	107.25(12)
N(2)–M(1)–O(2)	—	106.86(7)	111.61(10)	160.41(13)	87.95(12)
M(1)–N(1)–Si(1)	—	—	92.75(11)	95.34(15)	94.77(15)
M(1)–N(2)–Si(1)	—	123.18(10)	90.60(11)	93.31(15)	94.90(16)
N(2)–Si(1)–N(2)	104.15(8)	—	99.43(12)	101.88(16)	104.10(19)

[a] M = Mg. [b] M = Ca. [c] M = Sr.

Table 6 Turnover frequencies (298 K) and activation parameters for the catalytic dehydrocoupling of Et_2NH and Ph_2SiH_2

Catalyst	TOF (h^{-1})	E_a (kcal mol^{-1})	$\Delta H^{\ddagger}$ (kcal mol^{-1})	$\Delta S^{\ddagger}$ (cal mol^{-1} K^{-1})	$\Delta G^{\ddagger}_{298}$ (kcal mol^{-1})
1	57.1(4)	14.6(2)	13.9(2)	−29.8(6)	22.8
2	2822.5(54)	7.4(1)	6.8(1)	−46.8(1)	20.7
3	125.5(22)	11.2(23)	10.6(23)	−41.2(81)	23.5

the basicity and resultant ability of the group 2 amide or alkyl pre-catalyst to effect deprotonation of primary or secondary amine substrates.[34,35] In the current instance it appears that the relative ease of Si–H/M–N or N–H/M–N metathesis is a further significant consideration affected by the identity of the specific group 2 pre-catalyst and co-ligand employed. Furthermore, the persistence of $HN(SiMe_3)_2$ in the reaction medium during catalysis using compounds **1** and **3** is, unlike the $Ph_2SiHN(SiMe_3)_2$ produced during initiation of **2**, likely to have an inhibitory effect on the reaction and may account, at least in part, for the increased activity of calcium relative to the other congeners in these reactions.

While these observations and the first order rate dependence on [**1**] (*vide supra*) suggest that a monomeric constitution may be maintained through persistent hexamethyldisilazide ligation of magnesium, the origin of a similar rate dependence for calcium but second order behaviour with respect to [**3**] is less readily ascribed. We have earlier suggested that a second order rate dependence on [catalyst] in group 2-based processes is suggestive of a dimeric active catalytic centre,[34b,35] which generally results in the case of the larger heavier alkaline earth dications. Although the apparently differing modes of pre-catalyst activation are probably significant, in the absence of further corroborative evidence, we surmise that the current data are a result of similar variations in solution molecularity.

Arrhenius and Eyring analyses provided activation parameters (Table 6) for the reactions depicted in Scheme 4 which are commensurate with the superior activity provided by compound **2**. Although the calcium-based process enjoys an advantage of some 4–8 kcal mol^{-1} in its calculated activation energy and enthalpy of activation, the resultant $\Delta G^{\ddagger}_{298}$ values for the three group 2 systems are less indicative of such significant discrimination in reaction rates. Similar activation parameters as those derived here for catalysis by **2** and a deduced zero order dependence upon [amine] (eqn (1)) led Sadow to propose that dehydrocoupling catalysis of $^tBuNH_2$ and $PhMeSiH_2$ by **III**, occurs *via* rate-determining nucleophilic attack by an intermediate magnesium amide on silicon to form a five-coordinate silicon centre (Scheme 2).[28] While the first order dependence on [amine] depicted in eqn (2) and (3) does not allow us to discount a similar mechanism in reactions catalysed by the simple homoleptic bis(trimethyl)amide derivatives, **1–3**, our observations suggest that different mechanisms are likely to be active across the various catalytic systems; an observation that is further corroborated by the observed divergence in activity for aniline dehydrocoupling between **III** and **1–3**. For example, while it would appear that a single bis(trimethylsilyl)amide remains bound to Mg during catalysis with compound **1**, this in itself is insufficient to replicate the behaviour dictated by the tris(oxazolinyl)borate ancillary ligand of **III**. Notably, a similar ligand-dependent behaviour has only very recently been established in the more widely considered area of group 2-based alkene hydroamination catalysis.[36] We have previously hypothesised that similar variations in the rates of reactions of these latter catalytic systems are a consequence of the differing charge densities of the M^{2+} cations and their resultant ability to mediate metathesis and C=C insertion.[35] A similar rationale has been proposed to account for differences in the ability of group 2 cations to engage in amine–borane dehydrocoupling[25] and comparable effects may indeed be the origin of the variations in the E_a and $\Delta H^{\ddagger}$ values of Table 6. The similarity of the free energy values for the reactions catalysed by **1–3** are a consequence of the negative entropy of activation (−46.8(1) cal mol^{-1} K^{-1}) associated with the calcium-based catalysis. We have previously reported that an entropic component can play a major role in deterministic kinetic analyses of group 2-based inter- and intramolecular alkene hydroamination and intramolecular alkyne hydroalkoxylation catalysis.[35] In the current case, however, it is likely that catalyst solution molecularity, mode of activation and a potential for the establishment of transaminative pre-equilibria between the amine substrate and $HN(SiMe_3)_2$ play an equally significant role in the relative efficacy of each individual catalysis.

Although it would be imprudent to attempt to present a definitive interpretation of these variations, with this caveat in place it is possible to draw some tentative conclusions regarding the transition in mechanism of the individual reactions. For magnesium and calcium, the deduced rate laws (eqn (2)) suggest that protonolysis of the amine by the hydride formed in the Si–H/M–N σ-bond metathesis step is rate determining. While the energetics of this process should indeed be influenced by the charge density of the M^{2+} cation in question, the likely origin of this variation, *viz.* the increased radius of the Ca^{2+} centre, also has marked consequences for both the mode of pre-catalyst activation and the ordering of the protonolysis transition state. Furthermore, previous computational studies on group 2-mediated hydroamination have noted a marked decrease in the barrier to protonolysis down the group.[35a] Meaningful comparison is further complicated for the strontium system described by the rate law in eqn (3), in which case the kinetic data evidence mediation of the reaction *via* a catalytic dimer. The first order dependences in [amine] and [silane] for catalysis by **3** are redolent of equal involvement of Et_2NH and Ph_2SiH_2 in the rate determining step and suggest that the Si–H/Mg–N σ-bond metathesis step to yield a metal hydride is rate determining. While rapid amine protonolysis is also consistent with the apparent mode of activation of compound **3** during catalysis, the equally significant rate dependence on [amine] requires further consideration. We and others have previously suggested that rate determining C=C insertion in group 2-mediated hydroamination catalysis is assisted by the presence of further coordinated equivalents of the protic substrate within the coordination sphere of the catalytic

centre.[35,37] The lower charge density and larger radius of the Sr^{2+} centre may, thus, also be significant in its ability to provide a less constrained and labile platform for reaction.

In conclusion, we have shown that the readily available magnesium, calcium and strontium amides, $[M\{N(SiMe_3)_2\}_2]_2$, are active catalysts for the dehydrogenative coupling of silanes and amines. Stoichiometric studies have provided evidence for amide intermediates consistent with a stepwise mechanism predicated upon a sequence of metal-centred amine deprotonation and/or silane-based metathesis steps. While all three pre-catalysts studied displayed broad reactivity with a wide variety of amine and silane coupling partners, in most cases the calcium pre-catalyst, **2**, provided significantly superior activity to either of its magnesium- or strontium-based congeners. These empirical observations were borne out by a comparative kinetic study of the catalysed reaction between Et_2NH and Ph_2SiH_2 which also highlighted distinct and divergent catalytic behaviour between all three amide pre-catalysts studied herein as well as the recently reported borato-magnesium species, **III**.[28] While our interpretation of these data is inconclusive it is clear that the intrinsic character (coordinative unsaturation and molecularity, ancillary ligation, bond polarity and charge density) of the group 2 centre employed in the catalysis has a profound effect upon not only the efficacy but also the mode and mechanism of reaction. Distinct differences in reactivity are now emerging across the entire series of alkaline earths. It is clear, therefore, that compounds of these elements must always be judged on their own merits and are predisposed to display a more diverse chemistry than their historical treatment would imply. We are continuing in our attempts to identify the causes of these variations and to deconvolute their impacts upon chemical reactivity and catalysis.

X-ray crystallography

Data for **7**–**11** were collected at 150 K on a Nonius Kappa CCD diffractometer equipped with an Oxford Cryosystem low temperature device, using graphite monochromated MoKα radiation ($\lambda = 0.71073$ Å). Data were processed using the Nonius Software.[38] Structure solution, followed by full-matrix least squares refinement was performed using the programme suite X-SEED.[39] For compound **7**, H(1) and H(2), attached to N(1) and N(2) respectively, were located and refined at a distance of 0.98 Å from the relevant parent atoms. H(1A), attached to Si(1), was also located and refined without restraints. For compound **8**, the hydrogen atoms attached to Si(1) were located and refined subject to being similar distances from the parent. H(1) attached to N(1) was similarly located and refined at distance of 0.98 Å from the nitrogen. C(36) and C(37) were found to be disordered in a 50 : 50 ratio over two proximate sites. The C–C distances were, thus, refined with distance restraints in the associated THF molecule to assist convergence. For compound **9**, H(1a), attached to Si(1) was located and refined freely. Some disorder was present. In particular, C(36)/C(37) were disordered over 2 sites in a 50 : 50 ratio, while C(41) was similarly fragmented but in a 70 : 30 ratio. The unit cell was seen to contain 2 areas of diffuse solvent which could not be modelled in any plausible manner. Hence PLATON SQUEEZE was employed to treat these regions. Based on pre-PLATON electron density and the results for the SQUEEZE analysis, guest solvent was included in the asymmetric unit as ½ of a THF molecule. Although the data quality for compound **10** was poor, the crystal structure was unambiguous. The asymmetric unit contained one molecule of toluene solvent in addition to one molecule of the complex. H(1) was located and freely refined. Some THF carbons disordered in 55 : 45 ratio [C(36), C(37), C(39), C(40), C(41) and C(42)]. ADP restraints were applied to fractional occupancy atoms and distance restraints applied in disordered regions to assist convergence. For compound **11**, H(1), attached to Si(1), was located and freely refined. C(40) was disordered over two sites in a 70 : 30 ratio, while C(43)–C(46) were disordered in 50 : 50 ratio. Some ADP, C–O and C–C restraints used in disordered regions to assist convergence.

Acknowledgements

We thank the EPSRC and the University of Bath for funding.

Notes and references

1 (*a*) D. W. Stephan, *Angew. Chem., Int. Ed.*, 2000, **39**, 314; (*b*) T. J. Clark, K. Lee and I. Manners, *Chem.–Eur. J.*, 2006, **12**, 8634; (*c*) R. Waterman, *Curr. Org. Chem.*, 2008, **12**, 1322; (*d*) R. Waterman, *Dalton Trans.*, 2009, 18.

2 (*a*) L. D. Schwartz and P. C. Keller, *J. Am. Chem. Soc.*, 1972, **94**, 3015; (*b*) P. C. Keller, *J. Am. Chem. Soc.*, 1974, **96**, 3078; (*c*) P. C. Keller, *Inorg. Chem.*, 1975, **14**, 438; (*d*) P. C. Keller, *Inorg. Chem.*, 1975, **14**, 440.

3 (*a*) C. W. Hamilton, R. T. Baker, A. Staubitz and I. Manners, *Chem. Soc. Rev.*, 2009, **38**, 279; (*b*) A. Staubitz, A. P. M. Robertson, M. E. Sloan and I. Manners, *Chem. Rev.*, 2010, **110**, 4023.

4 J. Y. Corey, *Adv. Organomet. Chem.*, 2004, **51**, 1.

5 S. Greenberg and D. W. Stephan, *Chem. Soc. Rev.*, 2008, **37**, 1482.

6 (*a*) E. W. Corcoran, Jr and L. G. Sneddon, *Inorg. Chem.*, 1983, **22**, 182; (*b*) E. W. Corcoran, Jr and L. G. Sneddon, *J. Am. Chem. Soc.*, 1984, **106**, 7793; (*c*) E. W. Corcoran, Jr and L. G. Sneddon, *J. Am. Chem. Soc.*, 1985, **107**, 7446; (*d*) H. Braunschweig and F. Guethlein, *Angew. Chem., Int. Ed.*, 2011, **50**, 12613; (*e*) H. Braunschweig, C. Claes and F. Guethlein, *J. Organomet. Chem.*, 2012, **706–707**, 144; (*f*) H. Braunschweig, P. Brenner, R. D. Dewhurst, F. Guethlein, J. O. C. Jimenez-Halla, K. Radacki, J. Wolf and L. Zöllner, *Chem.–Eur. J.*, 2012, **18**, 8605; (*g*) H. C. Johnson, C. L. McMullin, S. D. Pike, S. A. Macgregor and A. S. Weller, *Angew. Chem., Int. Ed.*, 2013, DOI: 10.1002/anie.201304382, in press.

7 (*a*) P. P. Power, *Nature*, 2010, **463**, 171; (*b*) T. Chivers and J. Konu, *Comments Inorg. Chem.*, 2009, **30**, 131.

8 See, for example; (*a*) T. Hayashi, *Acc. Chem. Res.*, 2000, **33**, 354; (*b*) B.-H. Kim, M.-Y. Cho and H.-G. Woo, *Synlett*, 2004, 761.

9 *Modern Reduction Methods*, ed. P. G. Andersson and I. J. Munslow, Wiley-VCH, Weinheim, 2008.

10 *Organotransition Metal Chemistry: from bonding to catalysis*, ed. J. F. Hartwig, University Science Books, Sausalito, Ca, 2010.
11 G. A. Molander and J. A. C. Romero, *Chem. Rev.*, 2002, **102**, 2161.
12 (*a*) C. A. Roth, *Ind. Eng. Chem. Prod. Res. Dev.*, 1972, **11**, 134; (*b*) Y. Tanabe, M. Murakami, K. Kitaichi and Y. Yoshida, *Tetrahedron Lett.*, 1994, **35**, 8409; (*c*) Y. Tanabe, T. Misaki, M. Kurihara, A. Iida and Y. Nishii, *Chem. Commun.*, 2002, 1628.
13 A. P. Smith, J. J. S. Lamba and C. L. Fraser, *Org. Synth.*, 2002, **78**, 82.
14 Y. D. Blum, K. B. Schwartz and R. M. Laine, *J. Mater. Sci.*, 1989, **24**, 1707.
15 (*a*) C. Eaborn, *Organosilicon Compounds*, Butterworths, London, 1960; (*b*) R. Fessenden and J. S. Fessenden, *Chem. Rev.*, 1961, **61**, 361; (*c*) V. Passarelli, G. Carta, G. Rossetto and P. Zanella, *Dalton Trans.*, 2003, 413.
16 L. H. Sommer and J. D. Citron, *J. Org. Chem.*, 1967, **32**, 2470.
17 H. Q. Liu and J. F. Harrod, *Organometallics*, 1992, **11**, 822.
18 E. Matarasso-Tchiroukhine, *J. Chem. Soc., Chem. Commun.*, 1990, 681.
19 H. Q. Liu and J. F. Harrod, *Can. J. Chem.*, 1992, **70**, 107.
20 (*a*) J. A. Reichl and D. H. Berry, *Adv. Organomet. Chem.*, 1998, 197; (*b*) W. D. Wang and R. Eisenberg, *Organometallics*, 1991, **10**, 2222.
21 (*a*) Y. Blum and R. M. Laine, *Organometallics*, 1986, **5**, 2081; (*b*) C. Biran, Y. D. Blum, R. Glaser, D. S. Tse, K. A. Youngdahl and R. M. Laine, *J. Mol. Catal.*, 1988, **48**, 183.
22 (*a*) K. Takaki, T. Kamata, Y. Miura, T. Shishido and K. Takehira, *J. Org. Chem.*, 1999, **64**, 3891; (*b*) K. Takaki, K. Komeyama and K. Takehira, *Tetrahedron*, 2003, **59**, 10381; (*c*) W. Xie, H. Hu and C. Cui, *Angew. Chem., Int. Ed.*, 2012, **51**, 11141. See also, (*d*) Y. Chen, H. Song and C. Cui, *Angew. Chem., Int. Ed.*, 2010, **49**, 8958.
23 J. X. Wang, A. K. Dash, J. C. Berthet, M. Ephritikhine and M. S. Eisen, *J. Organomet. Chem.*, 2000, **610**, 49.
24 For reviews, see; (*a*) A. G. M. Barrett, M. R. Crimmin, M. S. Hill and P. A. Procopiou, *Proc. R. Soc. A*, 2010, **466**, 927; (*b*) S. Harder, *Chem. Rev.*, 2010, **110**, 3852.
25 (*a*) M. R. Crimmin, A. G. M. Barrett, M. S. Hill, P. B. Hitchcock and P. A. Procopiou, *Organometallics*, 2007, **24**, 10410; (*b*) D. J. Liptrot, M. S. Hill, M. F. Mahon and D. J. MacDougall, *Chem.–Eur. J.*, 2010, **16**, 8508; (*c*) M. S. Hill, M. F. Mahon and T. P. Robinson, *Chem. Commun.*, 2010, **46**, 2498; (*d*) M. S. Hill, M. Hodgson, D. J. Liprot and M. F. Mahon, *Dalton Trans.*, 2011, **40**, 7783; (*e*) J. Spielmann, G. Jansen, H. Bandmann and S. Harder, *Angew. Chem., Int. Ed.*, 2008, **47**, 6290; (*f*) J. Spielmann and S. Harder, *J. Am. Chem. Soc.*, 2009, **131**, 5064; (*g*) J. Spielmann, M. Bolte and S. Harder, *Chem. Commun.*, 2009, 6934; (*h*) J. Spielmann, D. F.-J. Piesik and S. Harder, *Chem.–Eur. J.*, 2010, **16**, 8307; (*i*) P. Bellham, M. S. Hill, G. Kociok-Köhn and D. J. Liptrot, *Dalton Trans.*, 2013, **42**, 737; (*j*) P. Bellham, M. S. Hill, D. J. Liptrot, D. J. MacDougall and M. F. Mahon, *Chem. Commun.*, 2011, **47**, 9060; (*k*) P. Bellham, M. S. Hill, G. Kociok-Köhn and D. J. Liptrot, *Chem. Commun.*, 2013, **49**, 1960.
26 (*a*) M. S. Hill, M. F. Mahon and T. P. Robinson, *Chem. Commun.*, 2010, **46**, 2498; For a general review of dehydrocoupling catalysis by main group elements, see, (*b*) R. J. Less, R. L. Melen and D. S. Wright, *RSC Adv.*, 2012, **2**, 2191.
27 F. Buch and S. Harder, *Organometallics*, 2007, **26**, 5132.
28 J. F. Dunne, S. R. Neal, J. Engelkemier, A. Ellern and A. D. Sadow, *J. Am. Chem. Soc.*, 2011, **133**, 16782.
29 (*a*) P. B. Hitchcock, M. F. Lappert, G. A. Lawless and B. Royo, *J. Am. Chem. Soc.*, 1990, **30**, 96; (*b*) M. Westerhausen, *Inorg. Chem.*, 1991, **30**, 96.
30 M. R. Crimmin, A. G. M. Barrett, M. S. Hill, D. MacDougall, M. F. Mahon and P. A. Procopiou, *Chem.–Eur. J.*, 2008, **14**, 11292.
31 See, for example; (*a*) A. Xia, J. Heeg and C. H. Winter, *Organometallics*, 2002, **21**, 4718; (*b*) M. M. Olmstead, W. J. Grigsby, D. R. Chacon, T. Hascall and P. P. Power, *Inorg. Chim. Acta*, 1996, **251**, 273; (*c*) D. R. Armstrong, W. Clegg, R. E. Mulvey and R. E. Rowlings, *J. Chem. Soc., Dalton Trans.*, 2001, 409; (*d*) A. G. M. Barrett, I. J. Casely, M. R. Crimmin, M. S. Hill, J. R. Lachs, M. F. Mahon and P. A. Procopiou, *Inorg. Chem.*, 2009, **48**, 4445.
32 (*a*) W. Vargas, U. English and K. Ruhlandt-Senge, *Inorg. Chem.*, 2002, **41**, 5602; (*b*) L. T. Wendell, J. Bender, X. He, B. C. Noll and K. W. Henderson, *Organometallics*, 2006, **25**, 4953; (*c*) M. S. Hill, G. Kociok-Köhn and D. J. MacDougall, *Inorg. Chem.*, 2011, **50**, 5234.
33 (*a*) M. Veith, W. Frank, F. Tollner and H. Lange, *J. Organomet. Chem.*, 1987, **326**, 315; (*b*) C. Pi, L. Wan, Y. Gu, H. Wu, C. Wang, W. Zheng, L. Weng, Z. Chen, X. Yang and L. Wu, *Organometallics*, 2009, **28**, 5281; (*c*) D. Yang, Y. Ding, H. Wu and W. Zheng, *Inorg. Chem.*, 2011, **50**, 7698; (*d*) V. L. Blair, W. Clegg, A. R. Kennedy, Z. Livingstone, L. Russo and E. Hevia, *Angew. Chem., Int. Ed.*, 2011, **50**, 9857.
34 (*a*) M. R. Crimmin, M. Arrowsmith, A. G. M. Barrett, I. J. Casely, M. S. Hill and P. A. Procopiou, *J. Am. Chem. Soc.*, 2009, **131**, 9670; (*b*) M. Arrowsmith, M. R. Crimmin, A. G. M. Barrett, M. S. Hill, G. Kociok-Kohn and P. A. Procopiou, *Organometallics*, 2011, **30**, 1493; (*c*) A. G. Avent, M. R. Crimmin, M. S. Hill and P. B. Hitchcock, *Dalton Trans.*, 2005, 278.
35 (*a*) A. G. M. Barrett, C. Brinkmann, M. R. Crimmin, M. S. Hill, P. Hunt and P. A. Procopiou, *J. Am. Chem. Soc.*, 2009, **131**, 12906; (*b*) C. Brinkmann, A. G. M. Barrett, M. S. Hill and P. A. Procopiou, *J. Am. Chem. Soc.*, 2012, **134**, 2193; (*c*) C. Brinkmann, A. G. M. Barrett, M. S. Hill, P. A. Procopiou and S. Reid, *Organometallics*, 2012, **31**, 7287.
36 (*a*) M. Arrowsmith, M. S. Hill and G. Kociok-Köhn, *Organometallics*, 2011, **30**, 1291; (*b*) B. Liu, T. Roisnel, J.-F. Carpentier and Y. Sarazin, *Angew. Chem., Int. Ed.*, 2012, **51**, 4943.
37 J. F. Dunne, D. B. Fulton, A. Ellern and A. D. Sadow, *J. Am. Chem. Soc.*, 2010, **132**, 17680.
38 DENZO-SCALEPACKZ, Otwinowski and W. Minor, Processing of X-ray Diffraction Data Collected in Oscillation Mode, *Methods in Enzymology*, ed. C. W. Carter, Jr and R. M. Sweet, Academic Press, 1997, vol. 276: Macromolecular Crystallography, part A, pp. 307–326.
39 L. J. Barbour, X-Seed – A software tool for supramolecular crystallography, *J. Supramol. Chem.*, 2001, **1**, 189–191.

